

Widen the Resonance: Probing a New Regime of Neutrino Self-Interactions with Astrophysical Neutrinos

Isaac R. Wang^{1,*}, Xun-Jie Xu^{2,†} and Bei Zhou^{1,3,‡}

¹*Theory Division, Fermi National Accelerator Laboratory, Batavia, Illinois 60510, USA*

²*Institute of High Energy Physics, Chinese Academy of Sciences, Beijing 100049, China*

³*Kavli Institute for Cosmological Physics, University of Chicago, Chicago, Illinois 60637, USA*

(Dated: January 15, 2025)

Neutrino self-interactions beyond the standard model have profound implications in astrophysics and cosmology. In this work, we study an uncharted scenario in which one of the three neutrino species has a mass much smaller than the temperature of the cosmic neutrino background. This results in a relativistic component that significantly broadens the absorption feature on the astrophysical neutrino spectra, in contrast to the sharply peaked absorption expected in the extensively studied scenarios assuming a fully nonrelativistic cosmic neutrino background. By solving the Boltzmann equations for neutrino absorption and regeneration, we demonstrate that this mechanism provides novel sensitivity to sub-keV mediator masses, well below the traditional $\sim 1\text{--}100$ MeV range. Future observations of the diffuse supernova neutrino background with Hyper-Kamiokande could probe coupling strengths down to $g \sim 10^{-8}$, surpassing existing constraints by orders of magnitude. These findings open new directions for discoveries and offer crucial insights into the interplay between neutrinos and the dark sector.

Introduction.— Neutrinos, interacting feebly with matter, could strongly interact among themselves. This intriguing possibility, which is not only allowed by laboratory constraints [1–4] but also well-motivated from various beyond-the-standard-model (BSM) theories [5–10], has received growing interest in recent years—see, e.g., Ref. [11] for a review. Moreover, the cosmological and astrophysical implications of neutrino self-interactions are rich [12–33], with the most prominent ones related to CMB data interpretations [12–15], supernova dynamics [16–20], and astrophysical neutrino propagation [21–28].

Astrophysical neutrinos propagating through cosmic distances could be attenuated due to scattering with the cosmic neutrino background (CNB) via neutrino self-interactions [21–26]. To achieve observable attenuation, the mediator of neutrino self-interactions is often assumed to be light, typically around $m_\phi \sim 1\text{--}100$ MeV, with the coupling $g_\nu \sim 10^{-3}\text{--}10^{-1}$. The corresponding 4-Fermi effective interaction strength is $G_X \equiv g^2/m_\phi^2 \sim 10^5 G_F$ with G_F being the Fermi constant. Below the MeV scale, it is usually assumed that cosmological constraints (BBN and N_{eff}) do not allow any important effects on astrophysical neutrino propagation.

In this *Letter*, we propose an exceptionally interesting effect that could be exploited to probe a new regime of neutrino self-interactions *well below the MeV scale*. Compared to previous studies, our work takes into account a crucial factor that was neglected in the past but could substantially enhance the sensitivity reach. That is, the lightest neutrino species in the CNB today can still be

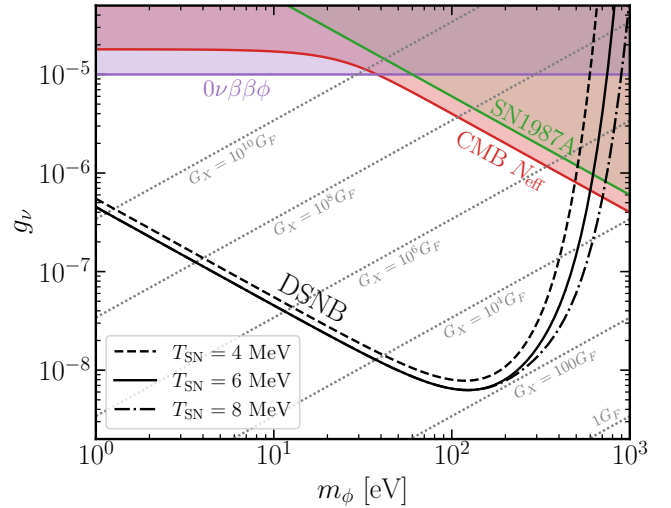


FIG. 1. The parameter space of neutrino self-interactions in the low-mass regime. The observation of DSNB in upcoming neutrino detectors such as Hyper-K can substantially improve current known bounds (shaded regions) by a few orders of magnitude (black lines).

relativistic, i.e., its mass being lower than the CNB temperature, which is allowed by all experimental data.

Fig. 1 presents a preview of our results. We demonstrate that future observations of the diffuse supernova neutrino background (DSNB) [34, 35] can probe m_ϕ of eV to sub-keV and g_ν down to 10^{-8} . This surpasses existing bounds by a few orders of magnitude. In terms of G_X , the best scenario may even reach $\mathcal{O}(100)G_F$.

Relativistic neutrinos may significantly enhance the absorption of astrophysical neutrinos during propagation. This occurs at the resonance of the s -channel scattering, $\nu\nu \rightarrow \phi \rightarrow \nu\nu$, where the mediator ϕ can be

* isaacw@fnal.gov

† xuxj@ihep.ac.cn

‡ beizhou@fnal.gov

either on- or off-shell. In previous studies [21–26], the CNB being scattered is assumed to be fully nonrelativistic. Thus, the resonance only occurs in a very narrow range of the astrophysical neutrino energy. In contrast, for relativistic CNB neutrinos that follow a thermal momentum distribution, the resonance can be reached at much wider energies. This is because each astrophysical neutrino with a certain momentum can always find a CNB neutrino with appropriate momentum such that their Mandelstam variable s matches m_ϕ^2 . In other words, *relativistic CNB neutrinos widen the resonance*, which is the key observation made in this letter.

The relativistic scenario becomes even more motivated after the recent DESI publication reporting the latest cosmological bound on the sum of neutrino masses [36, 37], as the upper bound is approaching the minimal value compatible with neutrino oscillation data [38]¹.

In the subsequent analysis, we estimate the absorption rate of DSNB neutrinos by the relativistic CNB to provide a qualitative discussion, highlighting the advantage of using such a scenario to probe neutrino self-interactions. To quantitatively study the impact on the DSNB, we perform a numerical computation by solving, for the first time, the Boltzmann equation for the coupled ν - ϕ system instead of that for ν only.

Interaction and mean-free path.— We consider the following Lagrangian for neutrino self-interactions:

$$\mathcal{L} \supset \frac{1}{2}(\partial\phi)^2 - \frac{1}{2}m_\phi^2\phi^2 + g_\nu\phi(\nu\nu + \nu^\dagger\nu^\dagger), \quad (1)$$

where ϕ is a real scalar and ν represents the two-component Weyl-van der Waerden spinor of a neutrino. Hence, Majorana neutrinos are implied by the Lagrangian. For simplicity, we do not consider the flavor structure in this Letter. A full flavor analysis will be conducted in our upcoming work.

With the interaction in Eq. (1), an astrophysical neutrino², ν_A , propagating through the CNB may scatter off a neutrino in the CNB, ν_C , via

$$\nu_A + \nu_C \rightarrow X, \quad X \in \{2\nu_A, \phi, 2\phi, \dots\}. \quad (2)$$

It is useful to introduce the mean-free path of the propagation, L_{mean} . In the ultra-relativistic (UR) and nonrelativistic (NR) scattering regimes, L_{mean} can be approximated as

$$L_{\text{mean}} \simeq \begin{cases} \left(\frac{g_\nu^2 m_\phi^2 T}{16\pi E_\nu^2} \exp\left[-\frac{m_\phi^2}{4TE_\nu}\right] + \dots \right)^{-1} & \text{(UR)} \\ (n_C \sigma_{\text{NR}})^{-1} & \text{(NR)} \end{cases}, \quad (3)$$

¹ If the cosmological bound further descends and becomes tension with the minimal value (see e.g. [39, 40]), then it might suggest that some mechanisms [41–44] render cosmic neutrinos lighter than those involved in oscillation measurements. In this case, more neutrino species in the CNB could be relativistic.

² Throughout this work, we use the term “astrophysical neutrinos” for neutrinos that acquire energies directly or indirectly from astrophysical sources. This includes neutrinos both emitted directly from such sources and regenerated through self-interactions.

where E_ν denotes the energy of the incoming ν_A , T the temperature of the CNB, n_C the number density of ν_C , and σ_{NR} denotes the NR cross section, which is almost independent of the momentum of ν_C . The UR and NR regimes correspond to the neutrino mass $m_\nu \ll T$ or $m_\nu \gg T$, respectively. For more general cases, L_{mean} can be derived from collision terms of Boltzmann equations—see the Supplemental Material. In the UR regime of Eq. (3), we only show the dominant contribution of $\nu_A + \nu_C \rightarrow \phi$, with “ \dots ” representing the remaining contributions. While in the NR regime, the contribution of $\nu_A + \nu_C \rightarrow \phi$ to σ_{NR} reads:

$$\sigma_{\text{NR}}^{(\text{res})} \simeq \pi g_\nu^2 \delta(s - m_\phi^2), \quad (4)$$

where $s \simeq 2E_\nu m_\nu$. Due to the δ -function, Eq. (4) gives rise to a very sharp and narrow absorption of ν_A by the CNB—see e.g. Fig. 1 of Ref. [21]. In practice, Eq. (4) is usually integrated into the resonance of s -channel scattering via the Breit–Wigner formalism (c.f. Eq. (25) in [45]), rather than being calculated separately.

In contrast to the narrow absorption in the NR regime, the absorption in the UR regime is much wider. As can be seen from Eq. (3), L_{mean}^{-1} in the UR regime peaks at $E_\nu \sim m_\phi^2/4T$, implying that ν_A of this energy can be absorbed most efficiently. If E_ν varies around this value by a factor of a few, the absorption is still effective.

Therefore, by comparing the NR and UR regimes, we see that *the most crucial difference is a very sharp and narrow absorption versus a much wider one*.

Taking the UR result with the present CNB temperature $T \simeq 1.9$ K and a few benchmark values indicated below, we find

$$\frac{L_{\text{mean}}}{1 \text{ Gpc}} \simeq 0.8 \left(\frac{10^{-8}}{g_\nu} \cdot \frac{E_\nu}{20 \text{ MeV}} \cdot \frac{0.1 \text{ keV}}{m_\phi} \right)^2 e^{-\lambda}, \quad (5)$$

where $\lambda \equiv \frac{m_\phi^2}{4TE_\nu}$ and for the above benchmark values it gives $e^{-\lambda} \sim \mathcal{O}(1)$. Obviously, the obtained L_{mean} for this benchmark is much shorter than the radius of the observable universe, $R_{\text{universe}} \simeq 14$ Gpc. This implies that the relativistic CNB over the entire universe would be opaque to a 20 MeV neutrino in the benchmark scenario! Therefore, observations of astrophysical neutrinos at such energies from sources that are cosmologically distant should be able to probe a sub-keV neutrino self-interaction mediator with $g_\nu \sim 10^{-8}$.

The above estimate of the mean free path serves as a qualitative study and has neglected the cosmological redshift. If ν_A is produced from high-redshift sources (e.g., redshift $z \sim 4 - 5$), it would propagate through a much denser and more energetic (hence more likely to be relativistic) neutrino background than the present CNB. A quantitative study, taking the cosmological redshift and other effects such as the production of ϕ and secondary ν_A into account, requires solving the Boltzmann equation, as we discuss below.

Solving the Boltzmann equation.— The Boltzmann equation that governs the evolution of the phase space

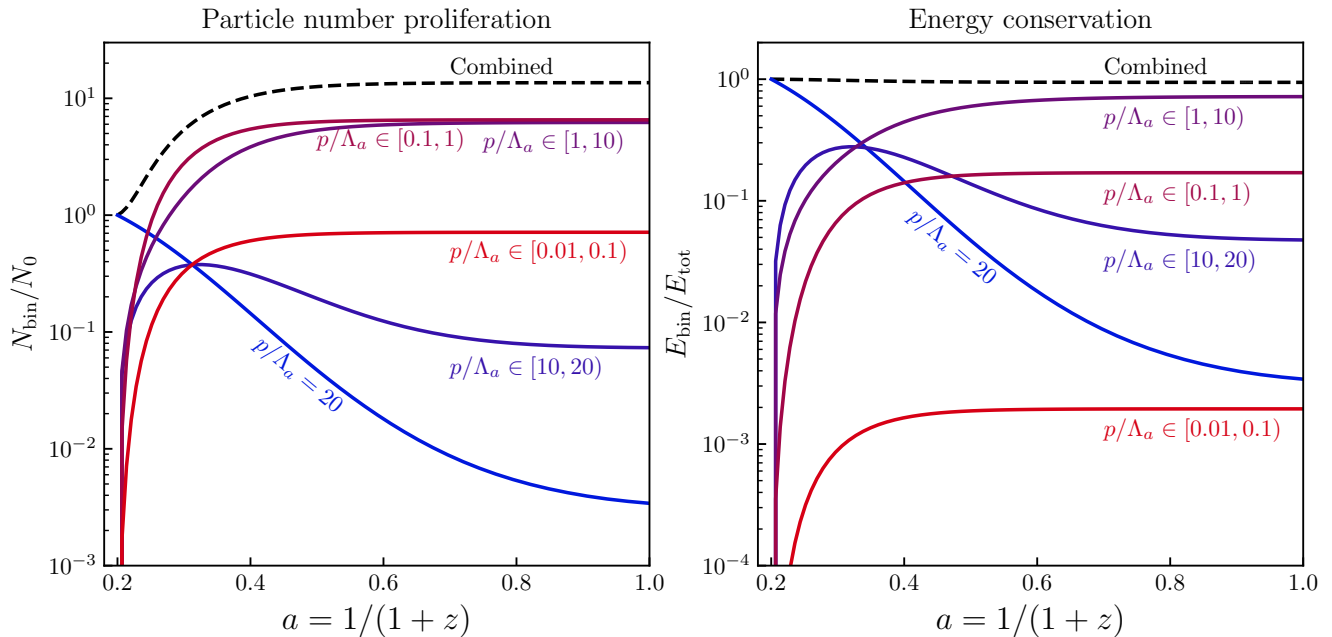


FIG. 2. Evolution of particle numbers (left) and energy (right), assuming $m_\phi = 100$ eV, $g_\nu = 6 \times 10^{-9}$, and a monochromatic and instantaneous source emitting neutrinos with $E_\nu = 20$ MeV at $z = 4$. Here, the monotonically decreasing curves represent neutrinos that retain their initial comoving momentum, corresponding to $p/\Lambda_a = 20$ where $\Lambda_a \equiv \text{MeV} \cdot a_i/a$. Other colored curves represent particles that are subsequently produced. The black dashed lines represent the total number and energy of these particles.

distributions of ν and ϕ in the expanding universe reads:

$$(\partial_t - H p \partial_p) \begin{bmatrix} f_\nu \\ f_\phi \end{bmatrix} = \begin{bmatrix} -f_\nu \Gamma_\nu^- + (1 - f_\nu) (\Gamma_\nu^+ + \mathcal{S}_\nu) \\ -f_\phi \Gamma_\phi^- + (1 + f_\phi) \Gamma_\phi^+ \end{bmatrix}, \quad (6)$$

where f_x is the phase space distribution of species $x = \nu$ or ϕ , $H = a^{-1} da/dt$ the Hubble parameter with a the scale factor, Γ_x^+ and Γ_x^- the production and depletion rates of x via particle physics processes such as those in Eq. (2), and \mathcal{S}_ν accounts for the production of ν from astrophysical sources.

In principle, f_ν could include both astrophysical and CNB neutrinos, with the former being viewed at a high-energy non-thermal addition to the thermal spectrum of the latter. However, the very hierarchical energy regimes between them and the low number density of the former make this treatment impractical. Hence, we separate the high-energy part from the thermal part and consider f_ν as the phase space distribution of ν_A only. Under this convention, we have $f_{\nu,\phi} \ll 1$, which implies that the Pauli-blocking and Bose-enhancement factors $1 \mp f_{\nu,\phi}$ can be neglected.

In the UR regime, the dominant processes contributing to $\Gamma_{\nu,\phi}^\pm$ are $\nu_A + \nu_C \rightarrow \phi$ and $\phi \rightarrow \nu_A + \nu_A$, with their contributions proportional to g_ν^2 . Other processes such as $\nu_A + \nu_C \rightarrow \nu_A + \nu_A$ (without resonance) and $\nu_A + \nu_C \rightarrow \phi + \phi$ are subdominant in the regime of our interest because their contributions are suppressed by g_ν^4 . In this work, we focus on the $\mathcal{O}(g_\nu^2)$ contributions, which can be

calculated analytically:

$$\Gamma_\nu^- = \frac{g_\nu^2 m_\phi^2 T}{16\pi E_\nu^2} \exp\left[-\frac{m_\phi^2}{4TE_\nu}\right], \quad (7)$$

$$\Gamma_\nu^+ = \frac{2g_\nu^2 m_\phi^2}{16\pi E_\nu^2} \int_{E_\phi^{\text{min}}}^{\infty} dE_\phi f_\phi, \quad (8)$$

$$\Gamma_\phi^+ = \frac{g_\nu^2 m_\phi^2}{16\pi E_\phi p_\phi} \int_{E_\nu^-}^{E_\nu^+} dE_\nu f_\nu \exp\left[-\frac{E_\phi - p_\nu}{T}\right], \quad (9)$$

$$\Gamma_\phi^- = \frac{g_\nu^2 m_\phi^2}{16\pi E_\phi}, \quad (10)$$

where E_ϕ and p_ϕ denote the energy and momentum of ϕ , $E_\phi^{\text{min}} = \frac{m_\phi^2}{4E_\nu} + E_\nu$, and $E_\nu^\mp = (E_\phi \mp p_\phi)/2$. With the analytical expressions of $\Gamma_{\nu,\phi}^\pm$ and a given source \mathcal{S}_ν , it is straightforward to solve the Boltzmann equation numerically.

Fig. 2 shows an example of a monochromatic and instantaneous source emitting neutrinos with $E_\nu = 20$ MeV at $z = 4$. In addition, we set $m_\phi = 100$ eV, $g_\nu = 6 \times 10^{-9}$ for neutrino propagation. The left and right panels show how the particle number and energy in each given momentum bin evolve, respectively. Here the particle number and energy in a bin are defined as $N_{\text{bin}} \equiv \int_{\text{bin}} \tilde{f}_{\nu+\phi}(\tilde{p}) \frac{d^3\tilde{p}}{(2\pi)^3}$ and $E_{\text{bin}} \equiv \int_{\text{bin}} \tilde{f}_{\nu+\phi}(\tilde{p}) \tilde{p} \frac{d^3\tilde{p}}{(2\pi)^3}$, where $\tilde{p} = ap$ is the comoving momentum and $\tilde{f}_{\nu+\phi}(\tilde{p}) \equiv f_\nu(p) + f_\phi(p)$. Note that our numerical computation

throughout the work uses much finer momentum binning than what is shown in the figure.

As is shown in the left panel, the total number of astrophysical neutrinos (black dashed line) increases rapidly after the initial production from the source. This is because $\nu_A + \nu_C \rightarrow \phi$ and $\phi \rightarrow \nu_A + \nu_C$ proceed efficiently at this stage. The two processes together lead to an exponential growth of ν_A with degraded energies, and meanwhile deplete ν_A at the initial energy. Despite the proliferation of the particle number, the total energy is approximately conserved (up to proper comoving factors), as is shown by the black dashed line in the right panel. The energy conservation rely on two approximations: (i) the energy contribution of ν_C is negligible, and (ii) the involved species are all relativistic³. The validity of (i) is guaranteed by the low temperature of CNB; and the validity of (ii) is implied by $E_\nu \gg m_\phi$. From the energy conservation and the particle number proliferation, we anticipate that the most prominent effect of neutrino self-interactions on the DSNB should be a substantial enhancement of its low-energy spectrum in combination with significant absorptions at high energies.

Impact on the DSNB spectrum. — To reach the resonance in the UR regime, E_ν needs to be around 1–100 MeV, which roughly matches the energy range of supernova neutrinos. Hence, the most suitable neutrino source to be considered in this work would be supernovae, provided that their distances are at the cosmological scale (Gpc). Although the neutrino flux of a single supernova at such a large distance is far from being observable in current and future experiments, the combined neutrino flux of all supernovae in the entire universe (i.e., DSNB) is likely to be detected in the foreseeable future [35]. Therefore, it is tempting to investigate whether and how the DSNB might be altered in the new physics scenario considered here.

The source term of the DSNB can be computed by [34, 35],

$$\mathcal{S}_\nu(E_\nu, a) = \frac{2\pi^2}{E_\nu^2} \cdot \frac{dN}{dE_\nu} \cdot \frac{R_{\text{SN}}}{a^3}, \quad (11)$$

where dN/dE_ν denotes the neutrino emission per supernova and R_{SN} is the rate of core-collapse supernova. Both can be approximated by analytical expressions and have been provided by Ref. [34]. Following the same setup in Ref. [34], we calculate Eq. (11) and substitute it into the Boltzmann equation. Solving the equation, we obtain the phase space distribution f_ν , which can be recast into the neutrino flux Φ_ν by

$$\Phi_\nu = a^3 \frac{E_\nu^2}{2\pi^2} f_\nu. \quad (12)$$

Fig. 3 shows the impact on the DSNB spectrum from neutrino self-interaction. In the upper panel, the black

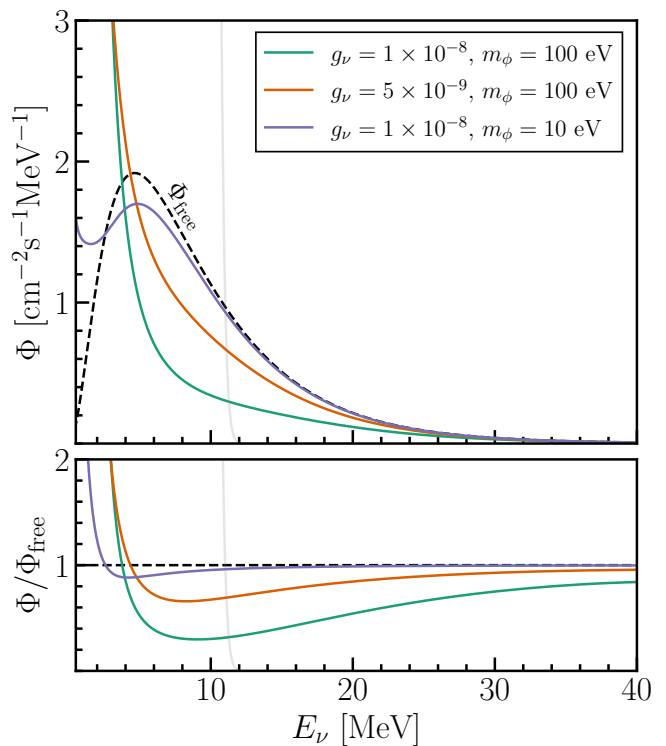


FIG. 3. The impact of neutrino self-interactions on the DSNB energy spectrum. *Upper panel:* neutrino flux. *Lower panel:* neutrino flux normalized by the result from the free propagation of DSNB neutrinos. The gray-shaded region indicates the background from reactor neutrinos [46, 47]. The solid curve indicates the free propagation of DSNB neutrinos. The DSNB temperature is assumed to be 6 MeV here.

dashed curve represents the DSNB neutrino flux without self-interactions, assuming a temperature of 6 MeV. This curve is confirmed to align with Fig. 4 in Ref. [34, 35] and is also approximately consistent with Fig. 1 in [47]. The colored curves depict the results of neutrino self-interaction. We show the combination of two different couplings, $g = 10^{-8}, 5 \times 10^{-9}$, with two different mediator masses $m_\phi = 10, 100$ eV. The lower panel illustrates the normalized results compared to free propagation, highlighting both creation and absorption effects. In all cases with the interaction, the neutrino flux in the MeV range is absorbed by $\nu_A + \nu_C \rightarrow \phi$. One can see the absorption in the lower panel behaves as a *wide dip*, indicating the result of the *widened resonance*. Next, the produced ϕ particles decay into two neutrinos, with each roughly carrying half of the energy of ν_A , given that CNB temperature is lower than ν_A energy by a few orders of magnitude. These created neutrinos further scatter with CNB to create more ϕ particles, which then decay into pairs of neutrinos with halved energies. Consequently, there is an accumulation of neutrinos in the low energy spectrum, leading to a blowing-up behavior in flux in the lower energy range, as shown in Fig. 3.

Detection and χ^2 analysis. — For DSNB detection,

³ Otherwise, there would be the dilution-resistant effect caused by the mass [31].

we focus on the dominant inverse beta decay (IBD) channel⁴ in the upcoming Hyper-Kamiokande (HK) detector that is expected to detect the DSNB with robust statistics due to its unprecedentedly large volume and excellent background reduction if it is Gadolinium doped. With a 3740 kt · yr exposure, HK is expected to detect ~ 800 DSNB events in the standard scenario above 12 MeV, while in the new physics scenario, the events above a certain energy could be substantially reduced.

To quantify the observability of the new physics effect, we adopt the following χ^2 function [48]:

$$\chi^2 = \left(\frac{y}{\sigma_y}\right)^2 + \sum_i \left(\frac{(1+y)N_i - N_{\text{st},i}}{\sigma_i}\right)^2, \quad (13)$$

where N_i and $N_{\text{st},i}$ denote the numbers of events in the i -th energy bin in the new physics and the standard model scenarios, respectively; y is a normalization factor; and σ_i and σ_y denote the uncertainties of N_i and y , respectively. With sufficient statistics ($N_{\text{st},i} \gg 1$), one can take $\sigma_i = \sqrt{N_{\text{st},i} + N_{\text{bkg},i}}$ where $N_{\text{bkg},i}$ is the number of background events. As the star formation rate used in the DSNB calculation may vary by roughly a factor of two [34], we consider a 50% uncertainty for the normalization ($\sigma_y = 0.5$) and marginalize a analytically—see e.g. [49]. The event numbers in HK are calculated following the same procedure in Ref. [28], with the background included in the same manner (see also Ref. [50] for a detailed study of the background).

Fig. 1 presents our projected sensitivity reach. We show explicitly that the result may vary slightly with the DSNB temperature T_{SN} for $m_\phi \lesssim 0.1$ keV. Above ~ 0.1 keV, the variation becomes much more significant. This uncertainty could be improved by better modeling of supernovae and ongoing observations of the DSNB in the future. In general, our result indicates that observations of DSNB at HK can probe neutrino self-interactions with m_ϕ from eV to sub-keV and g_ν down to 10^{-8} .

In the shown parameter space, there are a few existing bounds derived from the detection of SN1987A neutrinos [51–55], the cosmological parameter N_{eff} [31, 56], and neutrinoless double beta decay experiments searching for majoron emissions ($0\nu\beta\beta\phi$) [4, 57–60]. For the SN1987A bound, we adopt the most stringent one from Ref. [54]. For the N_{eff} bound, we take the bound on neutrinophilic scalar from Ref. [31], assuming that the allowed deviation of N_{eff} is less than 0.285 [61]. As for the $0\nu\beta\beta\phi$ bound, since m_ϕ here is well below the Q value of the process, it is almost independent of m_ϕ . Experimental searches typically set an upper bound on g_ν around 10^{-5} [57, 60].

Comparing our result with the existing bounds in Fig. 1, we see that a substantial part of the unexplored

parameter space can be probed by DSNB observations. In this work, we focus on supernova neutrinos mainly because the energy scale at $\mathcal{O}(10)$ MeV is ideal for the resonant production of sub-keV ϕ . Nevertheless, our calculation can be readily applied to other astrophysical sources at much higher energies. For instance, PeV or EeV neutrinos would allow us to explore the widened resonance for $m_\phi \sim 1$ or 30 MeV, respectively. We leave these interesting scenarios to future work.

Summary and conclusions.—Strong beyond-the-standard-model neutrino self-interactions are well-motivated and exhibit rich phenomena in astrophysics and cosmology. An intriguing consequence is that astrophysical neutrinos propagating through cosmic distances could be attenuated due to scattering with the CNB, typically resulting in a sharp absorption feature on the spectrum due to the resonance production of the mediator from the self-interaction. This mechanism provides stringent constraints on light mediators with masses of ~ 1 –100 MeV and coupling strengths in the range of 10^{-3} to 10^{-1} .

In this letter, we consider an uncharted scenario in which the absorption is broadened significantly due to a relativistic component of the CNB. This occurs if the mass of the lightest neutrino species is below the CNB temperature, which is allowed by neutrino-oscillation measurements and motivated by recent DESI data; thus, the CNB could follow a wide thermal momentum distribution, enabling a much wider range of astrophysical neutrino energies to satisfy the resonance condition.

We demonstrate that this broadened absorption feature offers a novel sensitivity to sub-keV mediator masses, well below the traditional 1–100 MeV range. By solving the Boltzmann equations for the coupled neutrino-mediator system, we quantitatively evaluate the absorption and regeneration of DSNB neutrinos during propagation. Our results show that for mediator masses in the eV to sub-keV range, future observations of the DSNB by Hyper-Kamiokande would have a sensitivity of the coupling strength up to $g \sim 10^{-8}$, surpassing existing constraints by a few orders of magnitude.

This scenario warrants various studies in future work. For example, the proliferation of sub-10 MeV neutrinos could exceed the fluxes of neutrinos from reactors and other sources. Furthermore, rich phenomenology could manifest in TeV–EeV astrophysical neutrinos observed by IceCube and other observatories. Altogether, they will significantly extend our reach in the parameter space of neutrino self-interactions, offering valuable insights into the mystery of neutrinos and their possible interplay with the dark sector.

Acknowledgement I. R. W. and B. Z. was supported by Fermi Research Alliance, LLC under Contract No. DE-AC02-07CH11359 with the U.S. Department of Energy, Office of Science, Office of High Energy Physics, and are currently supported by Fermi Forward Discovery Group, LLC under Contract No. 89243024CSC000002 with the U.S. Department of Energy, Office of Science,

⁴ Other neutrino detectors such as DUNE and JUNO may have their own advantages such as new detection channels other than IBD and the possibility of detecting the DSNB at lower energies.

Office of High Energy Physics. I. R. W. is also supported by DOE distinguished scientist fellowship grant FNAL 22-33. The work of X. J. X. is supported in part by the

National Natural Science Foundation of China (NSFC) under grant No. 12141501 and also by the CAS Project for Young Scientists in Basic Research (YSBR-099).

-
- [1] J. M. Berryman, A. De Gouvêa, K. J. Kelly, and Y. Zhang, “Lepton-Number-Charged Scalars and Neutrino Beamstrahlung,” *Phys. Rev. D* **97** (2018) no. 7, 075030, [arXiv:1802.00009 \[hep-ph\]](#).
- [2] N. Blinov, K. J. Kelly, G. Z. Krnjaic, and S. D. McDermott, “Constraining the Self-Interacting Neutrino Interpretation of the Hubble Tension,” *Phys. Rev. Lett.* **123** (2019) no. 19, 191102, [arXiv:1905.02727 \[astro-ph.CO\]](#).
- [3] V. Brdar, M. Lindner, S. Vogl, and X.-J. Xu, “Revisiting neutrino self-interaction constraints from Z and τ decays,” *Phys. Rev. D* **101** (2020) no. 11, 115001, [arXiv:2003.05339 \[hep-ph\]](#).
- [4] F. F. Deppisch, L. Graf, W. Rodejohann, and X.-J. Xu, “Neutrino Self-Interactions and Double Beta Decay,” *Phys. Rev. D* **102** (2020) no. 5, 051701, [arXiv:2004.11919 \[hep-ph\]](#).
- [5] Y. Chikashige, R. N. Mohapatra, and R. D. Peccei, “Are There Real Goldstone Bosons Associated with Broken Lepton Number?,” *Phys. Lett. B* **98** (1981) 265–268.
- [6] E. Ma, I. Picek, and B. Radovčić, “New Scotogenic Model of Neutrino Mass with $U(1)_D$ Gauge Interaction,” *Phys. Lett. B* **726** (2013) 744–746, [arXiv:1308.5313 \[hep-ph\]](#).
- [7] M. Lindner, D. Schmidt, and A. Watanabe, “Dark matter and $U(1)'$ symmetry for the right-handed neutrinos,” *Phys. Rev. D* **89** (2014) no. 1, 013007, [arXiv:1310.6582 \[hep-ph\]](#).
- [8] M. Berbig, S. Jana, and A. Trautner, “The Hubble tension and a renormalizable model of gauged neutrino self-interactions,” *Phys. Rev. D* **102** (2020) no. 11, 115008, [arXiv:2004.13039 \[hep-ph\]](#).
- [9] X.-J. Xu, “The ν_R -philic scalar: its loop-induced interactions and Yukawa forces in LIGO observations,” *JHEP* **09** (2020) 105, [arXiv:2007.01893 \[hep-ph\]](#).
- [10] G. Chauhan and X.-J. Xu, “How dark is the ν_R -philic dark photon?,” *JHEP* **04** (2021) 003, [arXiv:2012.09980 \[hep-ph\]](#).
- [11] J. M. Berryman *et al.*, “Neutrino self-interactions: A white paper,” *Phys. Dark Univ.* **42** (2023) 101267, [arXiv:2203.01955 \[hep-ph\]](#).
- [12] C. D. Kreisch, F.-Y. Cyr-Racine, and O. Doré, “Neutrino puzzle: Anomalies, interactions, and cosmological tensions,” *Phys. Rev. D* **101** (2020) no. 12, 123505, [arXiv:1902.00534 \[astro-ph.CO\]](#).
- [13] S. Roy Choudhury, S. Hannestad, and T. Tram, “Updated constraints on massive neutrino self-interactions from cosmology in light of the H_0 tension,” *JCAP* **03** (2021) 084, [arXiv:2012.07519 \[astro-ph.CO\]](#).
- [14] S. Roy Choudhury, S. Hannestad, and T. Tram, “Massive neutrino self-interactions and inflation,” *JCAP* **10** (2022) 018, [arXiv:2207.07142 \[astro-ph.CO\]](#).
- [15] J. Venzor, G. Garcia-Arroyo, J. De-Santiago, and A. Pérez-Lorenzana, “Resonant neutrino self-interactions and the H_0 tension,” *Phys. Rev. D* **108** (2023) no. 4, 043536, [arXiv:2303.12792 \[astro-ph.CO\]](#).
- [16] A. Das, A. Dighe, and M. Sen, “New effects of non-standard self-interactions of neutrinos in a supernova,” *JCAP* **05** (2017) 051, [arXiv:1705.00468 \[hep-ph\]](#).
- [17] S. Shalgar, I. Tamborra, and M. Bustamante, “Core-collapse supernovae stymie secret neutrino interactions,” *Phys. Rev. D* **103** (2021) no. 12, 123008, [arXiv:1912.09115 \[astro-ph.HE\]](#).
- [18] P.-W. Chang, I. Esteban, J. F. Beacom, T. A. Thompson, and C. M. Hirata, “Toward Powerful Probes of Neutrino Self-Interactions in Supernovae,” *Phys. Rev. Lett.* **131** (2023) no. 7, 071002, [arXiv:2206.12426 \[hep-ph\]](#).
- [19] D. F. G. Fiorillo, G. G. Raffelt, and E. Vitagliano, “Large Neutrino Secret Interactions Have a Small Impact on Supernovae,” *Phys. Rev. Lett.* **132** (2024) no. 2, 021002, [arXiv:2307.15115 \[hep-ph\]](#).
- [20] D. F. G. Fiorillo, G. G. Raffelt, and E. Vitagliano, “Supernova emission of secretly interacting neutrino fluid: Theoretical foundations,” *Phys. Rev. D* **109** (2024) no. 2, 023017, [arXiv:2307.15122 \[hep-ph\]](#).
- [21] K. C. Y. Ng and J. F. Beacom, “Cosmic neutrino cascades from secret neutrino interactions,” *Phys. Rev. D* **90** (2014) no. 6, 065035, [arXiv:1404.2288 \[astro-ph.HE\]](#). [Erratum: *Phys.Rev.D* 90, 089904 (2014)].
- [22] K. Ioka and K. Murase, “IceCube PeV–EeV neutrinos and secret interactions of neutrinos,” *PTEP* **2014** (2014) no. 6, 061E01, [arXiv:1404.2279 \[astro-ph.HE\]](#).
- [23] M. Bustamante, C. Rosenstrøm, S. Shalgar, and I. Tamborra, “Bounds on secret neutrino interactions from high-energy astrophysical neutrinos,” *Phys. Rev. D* **101** (2020) no. 12, 123024, [arXiv:2001.04994 \[astro-ph.HE\]](#).
- [24] I. Esteban, S. Pandey, V. Brdar, and J. F. Beacom, “Probing secret interactions of astrophysical neutrinos in the high-statistics era,” *Phys. Rev. D* **104** (2021) no. 12, 123014, [arXiv:2107.13568 \[hep-ph\]](#).
- [25] C. Creque-Sarbinowski, J. Hyde, and M. Kamionkowski, “Resonant neutrino self-interactions,” *Phys. Rev. D* **103** (2021) no. 2, 023527, [arXiv:2005.05332 \[hep-ph\]](#).
- [26] A. Das, Y. F. Perez-Gonzalez, and M. Sen, “Neutrino secret self-interactions: A booster shot for the cosmic neutrino background,” *Phys. Rev. D* **106** (2022) no. 9, 095042, [arXiv:2204.11885 \[hep-ph\]](#).
- [27] K. Akita, S. H. Im, and M. Masud, “Probing non-standard neutrino interactions with a light boson from next galactic and diffuse supernova neutrinos,” *JHEP* **12** (2022) 050, [arXiv:2206.06852 \[hep-ph\]](#).
- [28] A. B. Balantekin, G. M. Fuller, A. Ray, and A. M. Suliga, “Probing self-interacting sterile neutrino dark matter with the diffuse supernova neutrino background,” *Phys. Rev. D* **108** (2023) no. 12, 123011,

- arXiv:2310.07145 [hep-ph].
- [29] G.-y. Huang, T. Ohlsson, and S. Zhou, “Observational Constraints on Secret Neutrino Interactions from Big Bang Nucleosynthesis,” *Phys. Rev. D* **97** (2018) no. 7, 075009, arXiv:1712.04792 [hep-ph].
- [30] E. Grohs, G. M. Fuller, and M. Sen, “Consequences of neutrino self interactions for weak decoupling and big bang nucleosynthesis,” *JCAP* **07** (2020) 001, arXiv:2002.08557 [astro-ph.CO].
- [31] S.-P. Li and X.-J. Xu, “ N_{eff} constraints on light mediators coupled to neutrinos: the dilution-resistant effect,” *JHEP* **10** (2023) 012, arXiv:2307.13967 [hep-ph].
- [32] Q.-f. Wu and X.-J. Xu, “Shedding light on neutrino self-interactions with solar antineutrino searches,” *JCAP* **02** (2024) 037, arXiv:2308.15849 [hep-ph].
- [33] I. R. Wang and X.-J. Xu, “Imprints of light dark matter on the evolution of cosmic neutrinos,” *JCAP* **05** (2024) 050, arXiv:2312.17151 [hep-ph].
- [34] S. Horiuchi, J. F. Beacom, and E. Dwek, “The Diffuse Supernova Neutrino Background is detectable in Super-Kamiokande,” *Phys. Rev. D* **79** (2009) 083013, arXiv:0812.3157 [astro-ph].
- [35] J. F. Beacom, “The Diffuse Supernova Neutrino Background,” *Ann. Rev. Nucl. Part. Sci.* **60** (2010) 439–462, arXiv:1004.3311 [astro-ph.HE].
- [36] DESI Collaboration, A. G. Adame *et al.*, “DESI 2024 VI: Cosmological Constraints from the Measurements of Baryon Acoustic Oscillations,” arXiv:2404.03002 [astro-ph.CO].
- [37] L. Herold and M. Kamionkowski, “Revisiting the impact of neutrino mass hierarchies on neutrino mass constraints in light of recent DESI data,” arXiv:2412.03546 [astro-ph.CO].
- [38] I. Esteban, M. C. Gonzalez-Garcia, M. Maltoni, I. Martinez-Soler, J. a. P. Pinheiro, and T. Schwetz, “NuFit-6.0: updated global analysis of three-flavor neutrino oscillations,” *JHEP* **12** (2024) 216, arXiv:2410.05380 [hep-ph].
- [39] D. Wang, O. Mena, E. Di Valentino, and S. Gariazzo, “Updating neutrino mass constraints with background measurements,” *Phys. Rev. D* **110** (2024) no. 10, 103536, arXiv:2405.03368 [astro-ph.CO].
- [40] N. Craig, D. Green, J. Meyers, and S. Rajendran, “No νs is Good News,” *JHEP* **09** (2024) 097, arXiv:2405.00836 [astro-ph.CO].
- [41] R. Fardon, A. E. Nelson, and N. Weiner, “Dark energy from mass varying neutrinos,” *JCAP* **10** (2004) 005, arXiv:astro-ph/0309800.
- [42] D. B. Kaplan, A. E. Nelson, and N. Weiner, “Neutrino oscillations as a probe of dark energy,” *Phys. Rev. Lett.* **93** (2004) 091801, arXiv:hep-ph/0401099.
- [43] V. Barger, P. Huber, and D. Marfatia, “Solar mass-varying neutrino oscillations,” *Phys. Rev. Lett.* **95** (2005) 211802, arXiv:hep-ph/0502196.
- [44] M. Cirelli, M. C. Gonzalez-Garcia, and C. Pena-Garay, “Mass varying neutrinos in the sun,” *Nucl. Phys. B* **719** (2005) 219–233, arXiv:hep-ph/0503028.
- [45] T. M. P. Tait, “TASI Lectures on Resonances,” 2009. www.physics.uci.edu/~ttait/tait-TASI08.pdf.
- [46] M. Baldoncini, I. Callegari, G. Fiorentini, F. Mantovani, B. Ricci, V. Strati, and G. Xhixha, “Reference worldwide model for antineutrinos from reactors,” *Phys. Rev. D* **91** (2015) no. 6, 065002, arXiv:1411.6475 [physics.ins-det].
- [47] E. Vitagliano, I. Tamborra, and G. Raffelt, “Grand Unified Neutrino Spectrum at Earth: Sources and Spectral Components,” *Rev. Mod. Phys.* **92** (2020) 45006, arXiv:1910.11878 [astro-ph.HE].
- [48] Particle Data Group Collaboration, S. Navas *et al.*, “Review of particle physics,” *Phys. Rev. D* **110** (2024) no. 3, 030001.
- [49] M. Lindner, W. Rodejohann, and X.-J. Xu, “Coherent Neutrino-Nucleus Scattering and new Neutrino Interactions,” *JHEP* **03** (2017) 097, arXiv:1612.04150 [hep-ph].
- [50] B. Zhou and J. F. Beacom, “First detailed calculation of atmospheric neutrino foregrounds to the diffuse supernova neutrino background in Super-Kamiokande,” *Phys. Rev. D* **109** (2024) no. 10, 103003, arXiv:2311.05675 [hep-ph].
- [51] K. Choi and A. Santamaria, “Majorons and Supernova Cooling,” *Phys. Rev. D* **42** (1990) 293–306.
- [52] M. Kachelriess, R. Tomas, and J. W. F. Valle, “Supernova bounds on Majoron emitting decays of light neutrinos,” *Phys. Rev. D* **62** (2000) 023004, arXiv:hep-ph/0001039.
- [53] Y. Farzan, “Bounds on the coupling of the Majoron to light neutrinos from supernova cooling,” *Phys. Rev. D* **67** (2003) 073015, arXiv:hep-ph/0211375.
- [54] D. F. G. Fiorillo, G. G. Raffelt, and E. Vitagliano, “Strong Supernova 1987A Constraints on Bosons Decaying to Neutrinos,” *Phys. Rev. Lett.* **131** (2023) no. 2, 021001, arXiv:2209.11773 [hep-ph].
- [55] S. Vogl and X.-J. Xu, “Heating the dark matter halo with dark radiation from supernovae,” arXiv:2411.18052 [hep-ph].
- [56] S. Sandner, M. Escudero, and S. J. Witte, “Precision CMB constraints on eV-scale bosons coupled to neutrinos,” *Eur. Phys. J. C* **83** (2023) no. 8, 709, arXiv:2305.01692 [hep-ph].
- [57] KamLAND-Zen Collaboration, A. Gando *et al.*, “Limits on Majoron-emitting double-beta decays of Xe-136 in the KamLAND-Zen experiment,” *Phys. Rev. C* **86** (2012) 021601, arXiv:1205.6372 [hep-ex].
- [58] T. Brune and H. Päs, “Massive Majorons and constraints on the Majoron-neutrino coupling,” *Phys. Rev. D* **99** (2019) no. 9, 096005, arXiv:1808.08158 [hep-ph].
- [59] K. Blum, Y. Nir, and M. Shavit, “Neutrinoless double-beta decay with massive scalar emission,” *Phys. Lett. B* **785** (2018) 354–361, arXiv:1802.08019 [hep-ph].
- [60] GERDA Collaboration, M. Agostini *et al.*, “Search for exotic physics in double- β decays with GERDA Phase II,” *JCAP* **12** (2022) 012, arXiv:2209.01671 [nucl-ex].
- [61] Planck Collaboration, N. Aghanim *et al.*, “Planck 2018 results. VI. Cosmological parameters,” *Astron. Astrophys.* **641** (2020) A6, arXiv:1807.06209 [astro-ph.CO]. [Erratum: *Astron. Astrophys.* 652, C4 (2021)].
- [62] S.-P. Li and X.-J. Xu, “Dark matter produced from right-handed neutrinos,” *JCAP* **06** (2023) 047, arXiv:2212.09109 [hep-ph].
- [63] K. Schmitz and X.-J. Xu, “Wash-in leptogenesis after the evaporation of primordial black holes,” *Phys. Lett. B* **849** (2024) 138473, arXiv:2311.01089 [hep-ph].

Widen the resonance: probe a new regime of neutrino self-interactions in astrophysical neutrinos

Supplemental Material

Isaac R. Wang, Xun-Jie Xu, and Bei Zhou

In this supplemental material, we present a detailed derivation of the collision terms involved in our Boltzmann equation and the discretization techniques to numerically solve the Boltzmann equation.

S1. COLLISION TERMS IN THE BOLTZMANN EQUATION

In this work, we are mainly concerned with two processes, $\nu_A + \nu_C \rightarrow \phi$ and $\phi \rightarrow 2\nu_A$. To simplify our notations, we denote the two processes by $1 + 2 \rightarrow 3$ and $1 + 2 \leftarrow 3$, where the numbers allow us to conveniently mark quantities of the corresponding particles. For instance, p_1 and E_3 denote the momentum of the first particle and the energy of the third particle in the two processes respectively. When associating these numbers to actual particles, particles 1 and 3 always refer to ν_A and ϕ , respectively, while particle 2 can be ν_C or ν_A , depending on whether it is in $1 + 2 \rightarrow 3$ or $1 + 2 \leftarrow 3$, respectively. For convenience, we also define the following notations:

$$d\Pi \equiv \frac{d^3p}{2E(2\pi)^3}, \quad \widetilde{dp} \equiv \frac{d^3p}{(2\pi)^3}. \quad (\text{S1})$$

As is well known, the collision terms of a Boltzmann equation typically involve multi-dimensional phase space integrals. In this work, we encounter the following integrals.

$$\Gamma_{\dot{1}+2\rightarrow 3} \equiv \frac{1}{2E_1} \int d\Pi_2 d\Pi_3 f_2 |\mathcal{M}|^2 (2\pi\delta)^4, \quad (\text{S2})$$

$$\Gamma_{\dot{1}+2\leftarrow 3} \equiv \frac{\xi}{2E_1} \int d\Pi_2 d\Pi_3 f_3 |\mathcal{M}|^2 (2\pi\delta)^4, \quad (\text{S3})$$

$$\Gamma_{1+2\rightarrow \dot{3}} \equiv \frac{1}{2E_3} \int d\Pi_1 d\Pi_2 f_1 f_2 |\mathcal{M}|^2 (2\pi\delta)^4, \quad (\text{S4})$$

$$\Gamma_{1+2\leftarrow \dot{3}} \equiv \frac{1}{2E_3} \int d\Pi_1 d\Pi_2 |\mathcal{M}|^2 (2\pi\delta)^4, \quad (\text{S5})$$

where f_i denotes the phase space distribution of the i -th particle, $|\mathcal{M}|^2$ is the squared amplitude of the process, and $(2\pi\delta)^4 \equiv (2\pi)^4 \delta^{(4)}(p_1 + p_2 - p_3)$. In Eq. (S3), we have introduced a parameter ξ which will be discussed later. In addition, we also add a small circle ($\dot{}$) on the top of particle 1 or 3 to indicate that the process is focused on this particle. For instance, $\Gamma_{\dot{1}+2\rightarrow 3}$ means the absorption rate of particle 1 via this process, while $\Gamma_{1+2\rightarrow \dot{3}}$ means the production rate of particle 3.

Note that in this work, the squared amplitude $|\mathcal{M}|^2$ is an energy-independent constant:

$$|\mathcal{M}|^2 = g_\nu^2 m_\phi^2.$$

More generally, the squared amplitude of a two-to-one or one-to-two process is usually a constant. Hence, to make our calculation applicable to more general cases, below we keep $|\mathcal{M}|^2$ without substituting its explicit form.

Since $|\mathcal{M}|^2$ is a constant, the phase space integration of Eq. (S5) can be straightforwardly performed, and we arrive at

$$\Gamma_{1+2\leftarrow \dot{3}} = \frac{|\mathcal{M}|^2}{16\pi E_3}, \quad (\text{S6})$$

which is exactly the boosted decay rate of particle 3.

Eq. (S2) requires the specific form of f_2 . Assuming $f_2 = \exp(-E_2/T)$, the phase space integration can also be performed analytically—see Appendix A.2. of Ref. [62] for more details. The result reads

$$\Gamma_{\dot{1}+2\rightarrow 3} = \frac{T|\mathcal{M}|^2}{16\pi E_1^2} \exp\left[-\frac{m_3^2}{4Tp_1}\right]. \quad (\text{S7})$$

Eq. (S4) involves two phase-space distributions, f_1 and f_2 . If both are thermal distributions, the phase space integration is also straightforward, and the result can be found in Ref. [62]. In our work, since we have a non-thermal neutrino flux scattering off a thermal background, we need to perform this integration with $f_2 = \exp(-E_2/T)$ while f_1 maintains an arbitrary form. In this circumstance, the integration cannot be fully carried out but can be reduced to a one-dimensional integral. More specifically, we first integrate out p_2 , leaving the energy-conservation part of the δ function to be integrated out later. Then we integrate out the azimuthal angle of p_1 , leading to

$$\Gamma_{1+2 \rightarrow \dot{3}} = \int (p_1^2 dp_1 f_1) f_2 \frac{1}{8E_1 E_2 E_3} \frac{1}{2\pi} \delta(E_1 + E_2 - E_3) |\mathcal{M}|^2 p_3^2 d \cos \theta_{13} \frac{dp_3}{dE_3}. \quad (\text{S8})$$

The next step would be to integrate out $\cos \theta_{13}$. As long as the energy of E_3 is kinematically allowed, there must be a value of $\cos \theta_{13}$ that hits the peak of the δ function. Thus, we can safely integrate out the δ function with this polar angle, arriving at

$$\Gamma_{1+2 \rightarrow \dot{3}} = \int (p_1^2 dp_1 f_1) f_2 \frac{1}{16\pi E_1 E_2 E_3} \frac{1}{\Delta} |\mathcal{M}|^2, \quad (\text{S9})$$

$$\Delta = \frac{p_1 p_3}{|E_3 - E_1|}. \quad (\text{S10})$$

Using $|E_3 - E_1| = E_2$ and $p_1 = E_1$, we arrive at

$$\Gamma_{1+2 \rightarrow \dot{3}} = \frac{g_\nu^2 m_\phi^2}{16\pi E_3 p_3} \int_{p_1^{\min}}^{p_1^{\max}} dp_1 f_1 \exp\left[-\frac{E_3 - p_1}{T}\right]. \quad (\text{S11})$$

Here the minimal and maximal values of p_1 are determined from energy-momentum conservation:

$$p_1^{\min} = \frac{E_3 - p_3}{2}, \quad p_1^{\max} = \frac{E_3 + p_3}{2}. \quad (\text{S12})$$

Using the same technique above, one can also reduce Eq. (S3) to

$$\Gamma_{\dot{1}+2 \leftarrow 3} = \frac{g_\nu^2 m_\phi^2}{16\pi E_1^2} \int_{E_3^{\min}}^{\infty} dE_3 f_3, \quad (\text{S13})$$

where

$$E_3^{\min} = \frac{m_\phi^2}{4p_1} + p_1. \quad (\text{S14})$$

The results of the above phase space integrals can be used to readily obtain the mean free path L_{mean} in Eq. (3). Since $\Gamma_{\dot{1}+2 \rightarrow 3}$ is the absorption rate of particle 1, it can be physically interpreted as the probability of the particle being absorbed by the medium per unit time, implying that before the absorption it can propagate through a mean distance of $v\langle t \rangle$ where $v = 1$ is the velocity for relativistic particle, and $\langle t \rangle = 1/\Gamma_{\dot{1}+2 \rightarrow 3}$. Using the result in Eq. (S7), we obtain the UR result in Eq. (3). For the NR case, we start from Eq. (S2) where f_2 now takes a nonrelativistic distribution. Then the $\int d\Pi_2 f_2$ part can be approximately replaced with $n_2/(2m_2)$, independent of the specific form of f_2 , and the remaining part gives rise to a quantity proportional to the cross section σ_{NR} . Combined together, we arrive at the NR result in Eq. (3).

Let us finally comment on the ξ factor in Eq. (S3). In this work, we take $\xi = 2$ to account for the fact that each ϕ decay generates two ν_A . Nevertheless, we would like to mention that in some new physics scenarios, it is possible to have $\xi = 1$. For instance, if ϕ is coupled to a standard model neutrino and a dark fermion χ (see e.g. [33]), then the propagation of χ should adopt $\xi = 1$ because each ϕ particle produce only one χ particle and each χ particle after scattering off a neutrino produces only one ϕ particle. This would lead to the conservation of the total particle number, which can be verified explicitly by the Boltzmann equation of their comoving number densities:

$$\frac{d}{a^3 dt} \begin{bmatrix} n_1 a^3 \\ n_3 a^3 \end{bmatrix} = \begin{bmatrix} -\int \widetilde{dp}_1 f_1 \Gamma_{\dot{1}+2 \rightarrow 3} + \int \widetilde{dp}_1 \Gamma_{\dot{1}+2 \leftarrow 3} \\ \int \widetilde{dp}_3 \Gamma_{1+2 \rightarrow \dot{3}} - \int \widetilde{dp}_3 \Gamma_{1+2 \leftarrow \dot{3}} f_3 \end{bmatrix}. \quad (\text{S15})$$

Summing the two rows together and substituting Eqs. (S2)-(S5) into it, we get $d(n_1 a^3 + n_3 a^3)/dt = 0$ if $\xi = 1$. If $\xi = 2$, the conservation of particle number does not hold, but the total energy density $\times a^4$ is approximately conserved if all species are relativistic.

S2. SOLVING THE BOLTZMANN EQUATION

When solving the Boltzmann equation of a phase space function f , it is useful to introduce the comoving momentum $\tilde{p} \equiv pa$ and the following variable transformation:

$$\begin{pmatrix} t \\ p \end{pmatrix} \rightarrow \begin{pmatrix} a \\ \tilde{p} \end{pmatrix}, \quad f \rightarrow \tilde{f} : \tilde{f}(a, \tilde{p}) = f(t, p), \quad (\text{S16})$$

This allows us to rewrite the standard form of the Boltzmann equation

$$\left[\frac{\partial}{\partial t} - Hp \frac{\partial}{\partial p} \right] f(t, p) = C^{(f)} \quad (\text{S17})$$

into the following form (see Appendix B of [62] for further details):

$$aH \frac{\partial}{\partial a} \tilde{f}(a, \tilde{p}) = C^{(f)} \Big|_{f \rightarrow \tilde{f}, p \rightarrow \tilde{p}/a}. \quad (\text{S18})$$

In many problems, the right-hand side of Eq. (S18) can be written into the form of $Y - \tilde{f}X$ where Y and X are some functions of a and \tilde{p} . Then Eq. (S18) can be solved analytically by computing some integrals of X and Y —see Sec. II of Ref. [25] and Appendix B of Ref. [63] for further details.

In our work, this analytical approach allows us to compute f_ν if only $\nu_A + \nu_C \rightarrow \phi$ is taken into account while the backreaction is neglected (which is physically possible if ϕ has a dominant decay width to other final states). Following the analytical approach in Ref. [25, 63], we obtain the following analytical result in the absence of the backreaction:

$$\tilde{f}_\nu(a, \tilde{p}) \approx \tilde{f}_\nu(a_i, \tilde{p}) \exp \left[\frac{a^{5/2} |\mathcal{M}|^2 T_0}{32\pi \tilde{p}^2 H_0 x^{5/4} \Omega_m^{1/2}} \Gamma \left(\frac{5}{4}, x \right) - C_i \right], \quad \text{with } x \equiv \frac{a^2 m_\phi^2}{4\tilde{p}T_0}. \quad (\text{S19})$$

Here a_i denotes the initial value of a , T_0 and H_0 denote the present value of T and H , Γ is an incomplete gamma function, and C_i is a constant that ensures the exponential reduces to 1 at $a = a_i$. When deriving this result, we have assumed $H = H_0 \sqrt{\Omega_\Lambda + \Omega_m/a^3} \approx H_0 \sqrt{\Omega_m/a^3}$, where $\Omega_\Lambda \approx 0.692$ and $\Omega_m \approx 0.308$ are the energy budgets of dark energy and matter in the present universe. This approximation is valid for $10^{-3} \lesssim a \lesssim 0.75$. Figure S1 shows the comparison of the analytical result in Eq. (S19) with the numerical solution (to be introduced later). They are indeed in excellent agreement when the universe is matter dominated.

In the presence of the backreaction, we need to solve Eq. (6), which can only be solved numerically. Our numerical approach is built upon the discretized momentum space:

$$\tilde{p} \rightarrow \tilde{\mathbf{P}} \equiv (\tilde{p}_1, \tilde{p}_2, \tilde{p}_3, \dots, \tilde{p}_n)^T, \quad (\text{S20})$$

$$\tilde{f} \rightarrow F \equiv [\tilde{f}(\tilde{p}_1), \tilde{f}(\tilde{p}_2), \tilde{f}(\tilde{p}_3), \dots, \tilde{f}(\tilde{p}_n)]^T. \quad (\text{S21})$$

Here and below, we use capital or bold-font letters (e.g. $\tilde{\mathbf{P}}$ and F) for some quantities to indicate that they are $n \times 1$ column vectors.

Next, we discretize and vectorize all momentum-dependent quantities in Eq. (6), which can be rewritten into the following matrix form:

$$\frac{d}{d \ln a} \begin{bmatrix} F_\nu \\ F_\phi \end{bmatrix} \approx \frac{1}{H} \begin{bmatrix} -B_{1+2 \rightarrow 3} & B_{1+2 \leftarrow 3} \\ B_{1+2 \rightarrow \dot{3}} & -B_{1+2 \leftarrow \dot{3}} \end{bmatrix} \begin{bmatrix} F_\nu \\ F_\phi \end{bmatrix} + \frac{1}{H} \begin{bmatrix} S_\nu \\ 0 \end{bmatrix}, \quad (\text{S22})$$

where those B 's are $n \times n$ matrices to be elucidated later and S_ν is the vectorized form of the source term:

$$S_\nu \equiv [S_\nu(\tilde{p}_1/a), S_\nu(\tilde{p}_2/a), S_\nu(\tilde{p}_3/a), \dots, S_\nu(\tilde{p}_n/a)]^T. \quad (\text{S23})$$

The B matrices are obtained by discretizing Eqs. (S6), (S7), (S11), and (S13):

$$(B_{1+2 \rightarrow 3})_{ii'} \approx \left(\frac{T |\mathcal{M}|^2}{16\pi \mathbf{E}_1^2} \exp \left[-\frac{m_3^2}{4T \mathbf{E}_1} \right] \right)_i \delta_{ii'}, \quad (\text{S24})$$

$$(B_{1+2 \leftarrow 3})_{ij} \approx \left(\frac{\xi |\mathcal{M}|^2}{16\pi \mathbf{E}_1^2} \right)_i \Theta_{ij}^{(\text{cond.1})} (\Delta \mathbf{E}_3)_j, \quad (\text{S25})$$

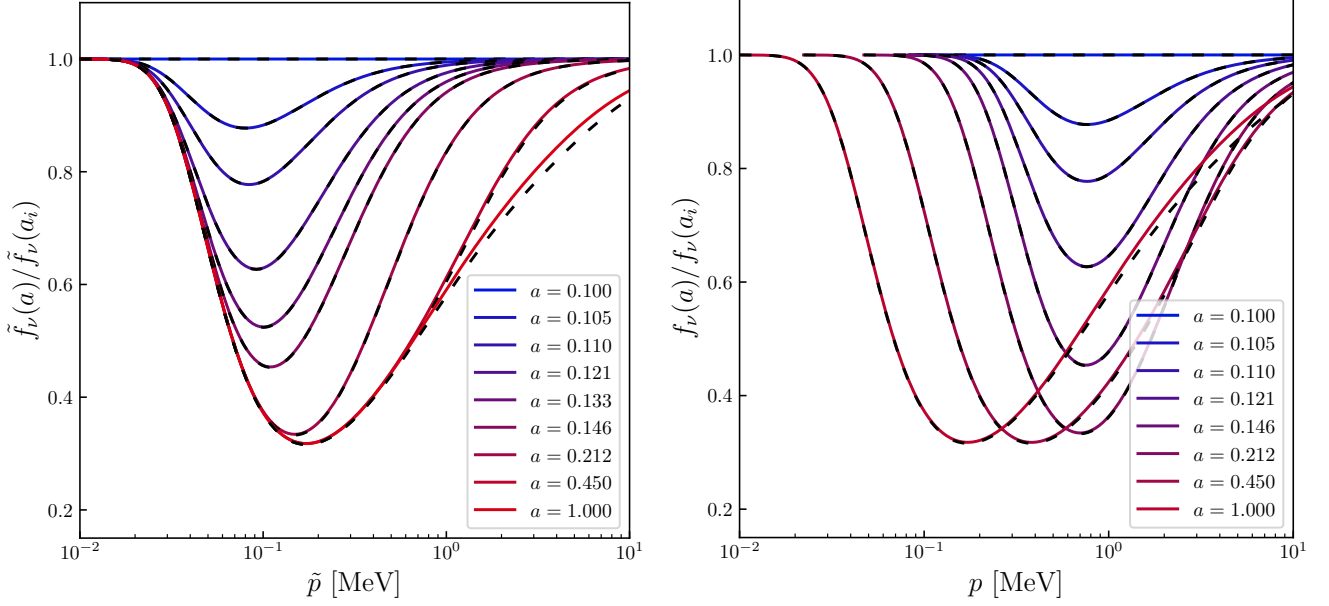


FIG. S1. Comparison of the analytical (dashed lines) and numerical (solid lines) results of solving the Boltzmann equation of f_ν , assuming only the presence of the absorption term. In this sample, we set $m_\phi = 10^2$ eV, $g = 10^{-9}$, and $a_i = 0.1$.

$$(B_{1+2\rightarrow\dot{3}})_{ji} \approx \left(\frac{|\mathcal{M}|^2}{16\pi \mathbf{E}_3 \mathbf{P}_3} e^{-\mathbf{E}_3/T} \right)_j \Theta_{ji}^{(\text{cond.2})} \left(\Delta_{\mathbf{P}_1} e^{\mathbf{P}_1/T} \right)_i, \quad (\text{S26})$$

$$(B_{1+2\leftarrow\dot{3}})_{jj'} \approx \left(\frac{|\mathcal{M}|^2}{16\pi \mathbf{E}_3} \right)_j \delta_{jj'}, \quad (\text{S27})$$

where $\Delta_{\mathbf{X}}$ denotes the bin width of the its subscript variable \mathbf{X} , corresponding to the discretized form of dX . Note that here \mathbf{E} and \mathbf{P} are not comoving quantities so when the system evolves using the fixed comoving grid of $\tilde{\mathbf{P}}$, they vary with a . The notation of Θ is defined as follows:

$$\Theta_{ij}^{(\text{cond.})} = \begin{cases} 1 & \text{if cond.} = \text{true} \\ 0 & \text{if cond.} = \text{false} \end{cases}, \quad (\text{S28})$$

with two specific conditions:

$$\text{cond.1} : \left(\frac{m_3^2}{4\mathbf{P}_1} + \mathbf{P}_1 \right)_i < (\mathbf{E}_3)_j, \quad (\text{S29})$$

$$\text{cond.2} : \left(\frac{\mathbf{E}_3 - \mathbf{P}_3}{2} \right)_j < (\mathbf{P}_1)_i < \left(\frac{\mathbf{E}_3 + \mathbf{P}_3}{2} \right)_j. \quad (\text{S30})$$

Assuming that ϕ is highly relativistic, we can further simplify Eqs. (S25) and (S26) into the following form:

$$(B_{\dot{1}+2\leftarrow 3})_{ij} \approx \left(\frac{\xi |\mathcal{M}|^2}{16\pi \mathbf{E}_1^2} \right)_i \theta_{i < j} (\Delta_{\mathbf{E}_3})_j, \quad (\text{S31})$$

$$(B_{1+2\rightarrow\dot{3}})_{ji} \approx \left(\frac{|\mathcal{M}|^2}{16\pi \mathbf{E}_3 \mathbf{P}_3} T \exp\left(-\frac{m_3^2}{4\mathbf{P}_3 T}\right) \right)_j \delta_{ji}. \quad (\text{S32})$$

where $\theta_{i < j} \equiv 1$ if $i < j$ and 0 if $i \geq j$. In practice, we find that using Eqs. (S31) and (S32) Eqs. (S25) and (S26) can greatly improve the numeric stability and performance of an ODE solver. Besides, Eq. (S22) allows one to conveniently implement the corresponding Jacobian to be fed into an ODE solver. We find that this can improve the speed of solving the equation typically by a factor of 10. On a generic laptop computer using the above method and the `scipy.integrate.solve_ivp` solver in python with the BDF method, it typically takes $\mathcal{O}(0.1)$ seconds to solve the discretized Boltzmann equation with $n = 300$. A small `atol` needs to be specified to achieve enough accuracy.